Behavioural Brain Research 371 (2019) 111978

Contents lists available at ScienceDirect

Behavioural Brain Research

journal homepage: www.elsevier.com/locate/bbr

Impairment of cognitive flexibility in type 2 diabetic *db/db* mice

Leonid M. Yermakov[a], Ryan B. Griggs[a], Domenica E. Drouet[a], Chiho Sugimoto[b], Michael T. Williams[b], Charles V. Vorhees[b], Keiichiro Susuki[a,*]

[a] Department of Neuroscience, Cell Biology, and Physiology, Boonshoft School of Medicine, Wright State University, Dayton, OH 45435, USA
[b] Department of Pediatrics, University of Cincinnati College of Medicine and Division of Neurology, Cincinnati Children's Research Foundation, Cincinnati, OH 45229, USA

ARTICLE INFO

Keywords:
Cognitive flexibility
Morris water maze
Axon initial segment
Node of Ranvier
Type 2 diabetes
db/db mice

ABSTRACT

Impaired executive function is a major peril for patients with type 2 diabetes, reducing quality of life and ability for diabetes management. Despite the significance of this impairment, few animal models of type 2 diabetes examine domains of executive function such as cognitive flexibility or working memory. Here, we evaluated these executive function domains in *db/db* mice, an established model of type 2 diabetes, at 10 and 24 weeks of age. The *db/db* mice showed impaired cognitive flexibility in the Morris water maze reversal phase. However, the *db/db* mice did not show apparent working memory disturbance in the spatial working memory version of the Morris water maze or in the radial water maze. We also examined axon initial segments (AIS) and nodes of Ranvier, key axonal domains for action potential initiation and propagation. AIS were significantly shortened in medial prefrontal cortex and hippocampus of 26-week-old *db/db* mice compared with controls, similar to our previous findings in 10-week-old mice. Nodes of Ranvier in corpus callosum, previously shown to be unchanged at 10 weeks, were elongated at 26 weeks, suggesting an important role for this domain in disease progression. Together, the findings help establish *db/db* mice as a model of impaired cognitive flexibility in type 2 diabetes and advance our understanding of its pathophysiology.

1. Introduction

Type 2 diabetes more than doubles the risk of dementia in older patients [1]. Even in patients with type 2 diabetes without dementia, cognitive dysfunction is a major concern during their lifespan [2]. Common cognitive impairments observed in patients with type 2 diabetes include decrement of long-term memory [3,4], cognitive flexibility [5,6], and working memory [7]. In addition to its negative impact on quality of life, diabetes-related cognitive dysfunction can exacerbate the course of the disease, since diabetes treatment relies on self-care capacity [8]. In particular, the executive function domains of cognitive flexibility and working memory are key for successful management of type 2 diabetes [9]. To study type 2 diabetes and its neurocognitive complications, rodent models such as *db/db* mice [10], Zucker Diabetic Fatty (ZDF) rats [11], and rodents given a high-fat diet [12] are commonly used. However, the majority of studies in these animals focused on two aspects of cognitive function: spatial learning and memory using the Morris water maze [13,14] and non-spatial memory using novel object recognition [15,16]. There are few studies in type 2 diabetic animals assessing cognitive flexibility and working memory, despite their significant impact on patients' life and diabetes management.

Among pathophysiologies implicated in neurological and psychiatric disorders, emerging evidence indicates the importance of alterations in the excitable axonal domains with highly accumulated voltage-gated sodium channels responsible for action potential initiation and propagation [17,18]. Structural characteristics of the axon initial segment (AIS), such as length and location, affect the excitability and firing behavior of neurons (reviewed in [19,20]). For example, rats exposed to a blast wave showed impaired memory on the novel object recognition task and decrease in the length of the AIS (1–4%) in hippocampus as well as in cortex, without physical impairment, motor deficits, brain cell death, or changes in brain injury markers [21]. A computational model showed that a shorter AIS (1–4%) reduces neuronal excitability and alters the interspike interval, suggesting that even subtle AIS shortening impacts neuronal function and therefore could be relevant to cognitive impairment [21]. Furthermore, experimental autoimmune encephalomyelitis, a mouse model of multiple sclerosis, showed AIS shortening in cortex [22] and impairments of working and long term memory irrespective of their motor performance [23]. Shortening of the

* Corresponding author at: Department of Neuroscience, Cell Biology, and Physiology, Boonshoft School of Medicine, Wright State University, 3640 Colonel Glenn Highway, Dayton, OH 45435, USA.
E-mail address: keiichiro.susuki@wright.edu (K. Susuki).

https://doi.org/10.1016/j.bbr.2019.111978
Received 10 January 2019; Received in revised form 23 May 2019; Accepted 24 May 2019
Available online 26 May 2019
0166-4328/

AIS length in the brain was also reported in a mouse model of Alzheimer's disease [24].

Similar to the AIS, voltage-gated sodium channels are highly accumulated at nodes of Ranvier and are responsible for the regeneration of action potentials [17,18]. At paranodes flanking both sides of the nodes, myelinating glial cells interact with axons to form junctions essential for node formation, maintenance, and function. Similar to AIS shortening [22], mice with experimental autoimmune encephalomyelitis showed alterations in nodes and paranodes in the optic nerves [25]. Paranodal disruption also was reported in ageing monkeys [26] and rats [27].

The mechanisms of cognitive dysfunction in type 2 diabetes remain unclear. Recently, we found that the AIS length is abnormally shortened in both prefrontal cortex and hippocampus of type 2 diabetic *db/db* mice at 10 weeks of age compared with control mice [28]. *Db/db* mice are leptin receptor-deficient [29] and closely mimic signs in patients with type 2 diabetes such as hyperinsulinemia, obesity, and progressive hyperglycemia [10,30]. Since shortening of the AIS length reduces neuronal excitability [21] and nodal elongation causes nerve conduction slowing [31], we hypothesized that cognitive dysfunction in type 2 diabetes is associated with structural changes at these domains. To test this idea, we analyzed cognitive function as well as AIS and nodal structures in type 2 diabetic *db/db* mice at different time points of disease progression, 10–15 weeks and 24–26 weeks of age.

2. Materials and methods

2.1. Animals

Male *db/db* (BKS.Cg-*Dock7*^{m} +/+ *Lepr*^{db}/J) mice (Jackson Laboratory, Bar Harbor, ME; RRID:IMSR_JAX:000642) aged 10–26 weeks were used. Age-matched heterozygote littermates (*db/+*) that are not diabetic were used as controls. Mice were housed in groups of three to four per cage at 22–24 °C with *ad libitum* access to food and water within the Laboratory Animal Resources at Wright State University under 12-h light/12-h dark conditions or in the AAALAC International accredited vivarium at Cincinnati Children's Research Foundation under 14-h light/10-h dark conditions. All animal procedures were approved by the Institutional Animal Care and Use Committee at Wright State University (Animal Use Protocol # 1113) or at Cincinnati Children's Research Foundation and conform to the United States Public Health Service Policy on Humane Care and Use of Laboratory Animals.

2.2. Behavioral testing experimental design

Behavioral testing was conducted at the Cincinnati Children's Research Foundation Animal Behavioral Core. Behavioral tests with 12–15 mice per group included Morris water maze (MWM) cued training (at 10 weeks of age), MWM spatial working memory version (at 10 weeks), radial water maze (at 11 weeks), MWM acquisition (at 12 weeks), MWM reversal (at 13 weeks), and open-field (at 15 weeks). MWM acquisition was repeated at 24 weeks, followed by MWM reversal at 25 weeks of age. MWM acquisition and reversal were followed by cued-random testing at 13 and 25 weeks of age. Mice could not be tested blindly because of observable differences in body weight; however, only radial water maze was scored manually. Open-field activity was quantified using an automated photobeam system and MWM cued training, spatial working memory, acquisition, reversal, and cued-random outcomes were scored by automated visual tracking software.

2.2.1. Open-field locomotor activity

Mice were tested for locomotor activity in photocell-based automated polycarbonate test chambers (41 cm × 41 cm × 30 cm, PAS system, San Diego Instruments, San Diego, CA). Mouse activity (total number of infrared beam interruptions) and ambulation (successive beam breaks) was recorded in 5 min intervals during a 1 h test period.

2.2.2. Morris water maze (MWM)

The test was performed as described [32] with modifications. A white 150 cm diameter polyethylene tank filled halfway with room temperature water (21 °C ± 1 °C) was used. A white platform was submerged 1.5 cm below the surface of the water, and the size of the platform varied depending on the test phase. Except for cued training and cued-random (during which a proximal cue was placed on the platform), curtains around the pool were opened so that distal cues (geometric shapes and posters on the walls) were visible. Mice were tested in rotation with the inter-trial interval determined by the number of mice being tested at any given time; however, the time was approximately 10 min. Latency to reach the platform and path efficiency (straight-line distance from start to platform ÷ the path taken by the mouse) to reach the goal, along with mean swim speed were measured using Any-Maze video tracking software (Stoelting Instruments, Wood Dale, IL).

2.2.2.1. MWM cued training. Cued training was given first to acclimate mice to the test requirements and assess swimming ability. Curtains were closed around the pool to obscure distal cues. The escape platform was 10 cm in diameter and contained an orange ball mounted on a steel rod 7 cm above the water to provide a proximal cue to the location of the platform. Mice were given six trials with fixed start and platform positions; latency to reach the goal was recorded.

2.2.2.2. MWM spatial working memory. To assess working memory, two trials per day were administered for 6 days. The location of a submerged 10 cm platform changed every day but did not change between trials, making the task a trial-dependent test of working memory. The first trial on each day was in a new location and represented the sample trial, during which the mouse learned the location of the platform by trial-and-error. The second, test trial, assessed the recollection of the platform location from the sample trial. Improvement of latency or path efficiency between trials 1 and 2 reflects working memory.

2.2.2.3. MWM acquisition. To assess spatial learning, the submerged platform acquisition phase spanned 5 days with 4 trials per day and a 60 s trial limit. Four quasi-random start positions were used. The submerged platform was 10 cm in diameter and remained in the same location during the 5 days of acquisition.

2.2.2.4. MWM reversal. To assess cognitive flexibility (i.e., the ability to extinguish the learned platform location used in acquisition and acquire a new location), the submerged platform was moved to the opposite quadrant from acquisition. A 7 cm diameter platform was used to increase task difficulty; the procedure was the same as acquisition, i.e., 4 trials/day for 5 days, but with different start positions.

2.2.2.5. MWM cued-random. To assess proximal cue learning, mice were tested in the MWM cued-random procedure. The 10 cm submerged platform was used but it was marked as during cued training with an orange ball mounted on a steel rod that extended 7 cm above the water. Curtains were closed around the pool to obscure distal cues. Whereas during cued training the start and platform were in a fixed location, for cued-random both the start and platform were moved on every trial such that no spatial strategy would be effective. Mice were given 4 trials per day for 2 days and latency to reach the platform was recorded.

2.2.3. Radial water maze (RWM)

To assess working memory, mice were tested using an 8-arm RWM [33]. A black 210 cm diameter polyethylene tank was filled halfway with room temperature water (21 °C ± 1 °C). There was a black 60 cm

diameter polyethylene octagon in the center requiring mice to choose an arm by swimming around the octagon. Posters were mounted around the room as distal cues. Each of the 8 arms of the maze was 55 cm long and 17 cm wide. At the start of each day, all arms had submerged platforms at the end except for the start arm. Mice were given 7 trials per day for 7 days. After the mouse was placed at the start arm, it was allowed to swim freely for 2 min. After a platform was found, the mouse was given a 30 s rest in a dry cage, and the found platform was removed. If the mouse failed to find a platform it was given a 2 min rest. An entry into an arm without a platform was counted as a working memory error. An entry into the start arm was counted as a reference memory error. An entry was defined as head and forelegs crossing an imaginary line at the entrance of an arm. The first day of testing in RWM was the training day to teach mice task requirements, therefore day 1 results were not used in the analyses.

2.3. Immunohistochemistry and measurements of AIS and nodes of Ranvier

Immunohistochemistry was performed as described [28]. In short, mice were sacrificed at 26 weeks of age by isoflurane overdose. Brains were rapidly dissected and fixed in ice-cold 4% paraformaldehyde for 90 min, cryoprotected overnight in 20% sucrose, and cryosectioned. Coronal brain sections (35 μm) were cut at 1.7 mm ± 0.15 mm (prefrontal cortex), 1.1 mm ± 0.20 mm (corpus callosum) and −1.64 mm ± 0.20 mm (hippocampus) relative to bregma. Free floating sections were blocked and incubated with primary antibody overnight at 4 °C, followed by staining with secondary antibodies at room temperature for 1 h. After mounting brain sections on microscope slides, three-dimensional z-stack images were taken of the prelimbic area of the medial prefrontal cortex at layers II/III and pyramidal layer of CA1 of the hippocampus using Axio Observer Z1 with Apotome 2 fitted with a Axiocam Mrm CCD camera (ZEISS, Thornwood, NY, USA). AIS length was measured using segmented line tool in Fiji [34], and nodal gap or paranodal length within the corpus callosum were measured using line tool in ZEN 2.3 (Zeiss). All measurements were performed by observers blinded to the identity of the images.

2.3.1. Antibodies

Primary antibodies were as follows: mouse monoclonal NeuN (1:4000 dilution; Millipore Cat# MAB377; RRID:AB_2298772), rabbit polyclonal Caspr (1:1500; Abcam Cat# ab34151; RRID:AB_869934), βIV spectrin (1:1500; M.N. Rasband, Baylor College of Medicine, TX, USA; RRID:AB_2315634), chicken polyclonal neurofascin (NF; 1:1500; R&D Systems Cat# AF3235; RRID:AB_10890736). Secondary antibodies were as follows: Alexa Fluor (594, 488, 350) or AMCA conjugated secondary antibodies (1:10,000 – 1:5000 dilution; Jackson ImmunoResearch Laboratories, West Grove, PA, USA). Hoechst 33342 (1:15,000 dilution; Cat# H3570, Thermo Fisher Scientific, IL, USA) was used for cell nuclei labeling.

2.4. Statistics

Behavioral data were analyzed using mixed linear ANOVA models (SAS Proc Mixed, SAS Institute 9.3, Cary, NC). Kenward-Roger adjusted degrees of freedom were used for these models. Diabetes was the between-subject factor and interval or day were the repeated measure factors. Significant diabetes-related interactions were further analyzed using slice-effect ANOVAs. One limitation of using Proc Mixed is that only a single repeated measure can be used in the model, therefore some analyses, such as for working memory, had separate analyses for each repeated measure. Data are presented as least square (LS) mean ± standard error of the mean (SEM). AIS and nodal data were analyzed using homoscedastic unpaired t-tests (2-tailed) and presented as mean ± SEM. An $\alpha = 0.05$ was used to determine statistical significance. Data were graphed using Prism 7.0 (GraphPad, La Jolla, CA, USA).

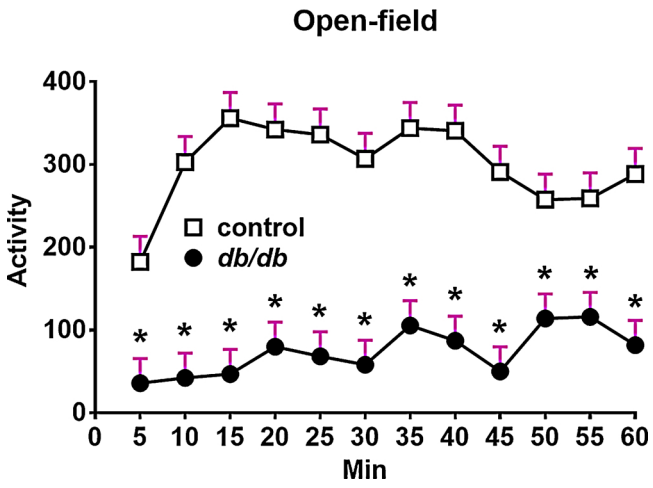

Fig. 1. Decreased locomotor activity of *db/db* mice during open-field test. Data collected in 5 min intervals over a span of 60 min. Data are LS Mean ± SEM. Group sizes: control = 12; *db/db* = 13. Mice were 15 weeks old at the time of testing. *$p \leq 0.05$ vs. control.

3. Results

3.1. Decreased locomotor activity in db/db mice

Previous studies showed significantly decreased locomotor activity of *db/db* mice starting by 10 weeks of age [35–39]. In our study, the open-field in 15-week-old mice showed a main effect of diabetes on activity ($F_{(1,\ 23.5)} = 49.23$, $p < 0.0001$) and a significant diabetes x interval interaction ($F_{(11,\ 199)} = 3.18$, $p = 0.0005$; Fig. 1). Similarly, there was a main effect of diabetes on ambulation ($F_{(1,\ 23.3)} = 47.65$, $p < 0.0001$) and a significant diabetes x interval interaction ($F_{(11,\ 205)} = 3.19$, $p < 0.0005$; not shown). These data support the idea raised by a previous study [35] that decreased locomotor activity of *db/db* mice could affect the interpretation of land-based tasks such as Y-maze. The cause of limited locomotor activity in *db/db* mice is unknown, but might be due to factors other than obesity [38]. Escape from water is relatively immune from activity or body mass differences [32]. Furthermore, swim path measurements in MWM do not correlate with swim speed or performance in land-based tasks [40]. Therefore, we decided to use water-based tasks to assess cognitive function in *db/db* mice.

3.2. MWM cued training

To teach mice to escape and assess swimming ability, MWM cued training was performed first. The *db/db* mice (37.3 ± 2.3 s, n = 15) took longer to locate the platform than the lean controls (26.0 ± 2.6 s, n = 12) ($F_{(1,\ 48.2)} = 10.77$, $p = 0.0019$). All mice improved over the 6 trials ($F_{(5,\ 90.1)} = 10.77$, $p = 0.0001$), although there was no interaction with diabetes. The increased latency to locate the platform in *db/db* mice compared with lean controls was likely due to their reduced swim speed (see Figs. 2B, 4 B,E). Therefore, to draw conclusions in the following MWM tests, we relied on the swim path efficiency, which is dimensionless [32].

3.3. Working memory assessment with MWM and RWM

Using spatial working memory version of the MWM similar to a previously reported method [41], we assessed working memory in *db/db* mice known to have diabetes [10] and AIS shortening in prefrontal cortex [28]. We found a main effect of diabetes on latency during Trial 1 ($F_{(1,\ 29.8)} = 11.89$, $p = 0.0017$) and Trial 2 ($F_{(1,\ 30.1)} = 20.70$, $p < 0.0001$; Fig. 2A) and a main effect of diabetes on swim speed during the

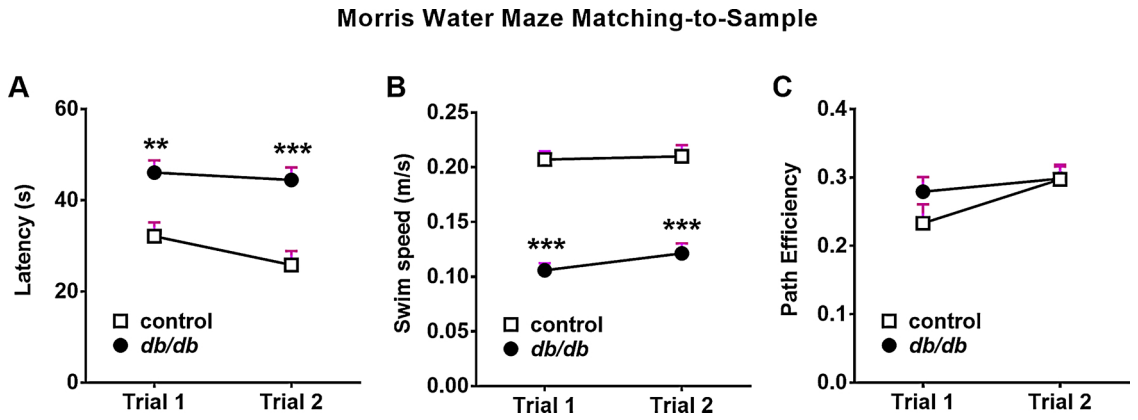

Fig. 2. MWM spatial working memory. (A) *Db/db* mice had significantly longer latencies than lean controls in both trials. (B) *Db/db* mice had significantly slower swim speeds in both trials. (C) There was no difference in path efficiency. All values are LS Mean ± SEM. Group sizes: control = 12; *db/db* = 15. Mice were 10 weeks old at the time of testing. $^{**}p < 0.01$, $^{***}p \leq 0.001$ when compared with controls.

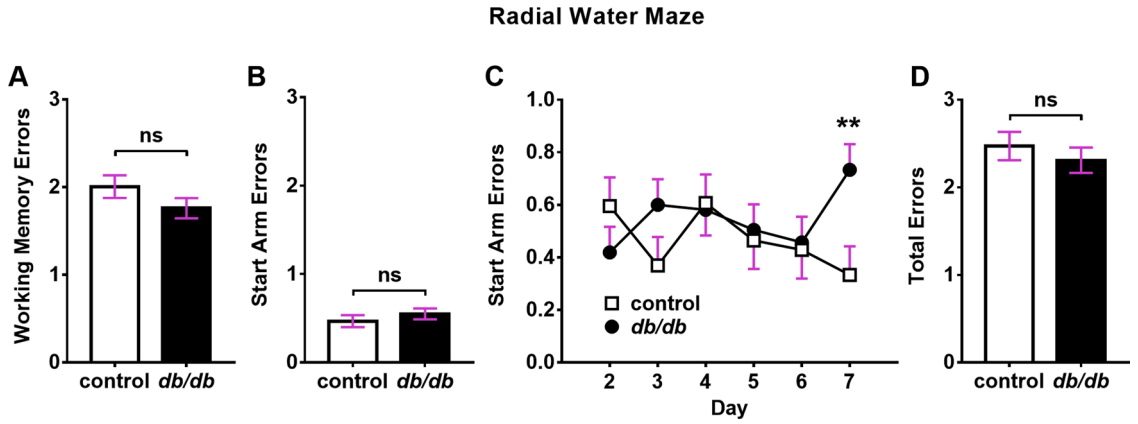

Fig. 3. Radial Water Maze. (A) Working memory errors across days for the lean controls and the *db/db* mice. (B) Start arm errors across days for the lean controls and the *db/db* mice. (C) Start arm errors by day for the lean controls and the *db/db* mice. *Db/db* mice had significantly more start arm errors on day 7 but not on days 2-6. (D) Total errors collapsed across days for the lean controls and the *db/db* mice. Data are LS Mean ± SEM. Mice were 11 weeks old at the time of testing. Group sizes: control = 12; *db/db* = 15. $^{**}p \leq 0.01$, vs. control. ns = not significant.

same trials (Trial 1: $F_{(1,\ 23.6)} = 107.02$, $p < 0.0001$; Trial 2: $F_{(1,\ 25.5)} = 42.11$, $p < 0.0001$; Fig. 2B). With the exception of swim speed on Trial 1, no effects of Day or the interaction of Diabetes x Day were observed for latency or swim speed. By contrast, path efficiency was not influenced by diabetes on Trials 1 or 2 (Fig. 2C); no performance improvement was observed between trials. There was no significant effect of Day or an interaction of Diabetes x Day for path efficiency. Similarly, RWM did not show a main effect of diabetes (Fig. 3A) or diabetes x day interaction for working memory errors. There was also no main effect of diabetes on start arm reference errors (Fig. 3B), but there was a diabetes x day interaction ($F_{(5,\ 81.8)} = 2.56$, $p = 0.0335$), with *db/db* mice making significantly more start arm reference memory errors on day 7 compared with lean controls (Fig. 3C). There was no main effect of diabetes (Fig. 3D) and no diabetes x day interaction for total errors on each day.

3.4. MWM spatial learning and flexibility at 12–14 weeks of age

To assess spatial learning in *db/db* mice, MWM acquisition was used (Fig. 4A–C). We found a significant main effect of diabetes on latency during acquisition ($F_{(1,\ 25.1)} = 30.64$, $p < 0.0001$), with no diabetes x day interaction (Fig. 4A). We also found a main effect of diabetes on swim speed ($F_{(1,\ 25)} = 200.25$, $p < 0.0001$), but no diabetes x day interaction (Fig. 4B). The *db/db* mice took longer to reach the platform and swam slower than the control mice. There were no main effects of diabetes or diabetes x day interaction on path efficiency during acquisition (Fig. 4C). To assess cognitive flexibility, we tested the mice on MWM reversal (Fig. 4D–F). There was a main effect of diabetes on latency ($F_{(1,\ 27.6)} = 46.73$, $p < 0.0001$) and a significant diabetes x day interaction ($F_{(4,\ 77.8)} = 2.68$, $p < 0.0001$; Fig. 4D), with *db/db* mice taking longer to locate the platform than controls on all days. There was a main effect of diabetes on swim speed ($F_{(1,\ 25.1)} = 185.91$, $p < 0.0001$) with the *db/db* mice swimming slower than controls, but no diabetes x day interaction (Fig. 4E). There was a main effect of diabetes ($F_{(1,\ 26)} = 7.39$, $p = 0.0115$) and diabetes x day interaction ($F_{(4,\ 82.4)} = 2.98$, $p = 0.0236$; Fig. 4F) for path efficiency. The *db/db* mice were less efficient than the lean controls on days 4 and 5 of reversal. At the end of reversal in 14-week-old mice, cued-random testing was performed. There was a significant diabetes effect on latency ($F_{(1,\ 25)} = 12.25$, $p = 0.0018$; not shown) with *db/db* mice taking longer to reach the cued platform than lean controls.

3.5. AIS length is reduced in prefrontal cortex and hippocampus of 26-week-old db/db mice

Age-dependent deterioration of cognitive function and brain pathology was described in *db/db* mice [38]. We previously reported AIS shortening in prefrontal cortex and hippocampus of 10-week-old *db/db* mice [28]. To test if prolonged disease affects AIS shortening, we evaluated prefrontal cortex (Fig. 5A–C) and hippocampus (Fig. 5D–F) of 26-week-old *db/db* mice. AIS length was shorter (11.2%) in *db/db* mice (23.87 ± 0.70 μm, n = 4) compared with controls (26.87 ± 1.00 μm,

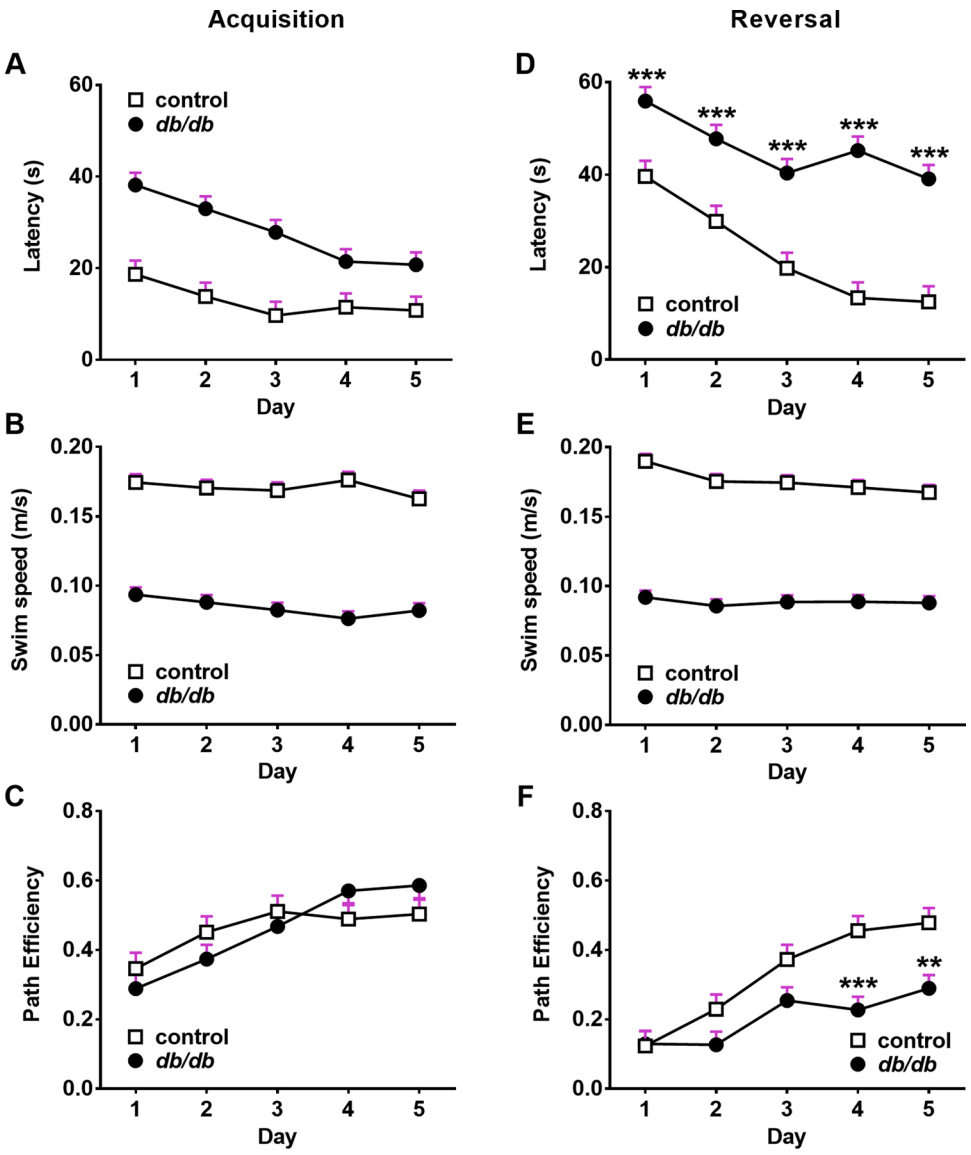

Fig. 4. MWM Acquisition (A–C) and Reversal (D–F). (A) *Db/db* mice had significantly longer latencies to reach the platform than lean controls. (B) Swim speed stayed constant during acquisition. (C) Path efficiency was similar in control and *db/db* mice on days 1–5 of acquisition. (D) *Db/db* mice had significantly longer latencies to reach the platform than lean controls. (E) Swim speed stayed constant during reversal. (F) Path efficiency was decreased in *db/db* mice compared with controls on days 4 and 5. Data are LS Mean ± SEM. Group sizes: control = 12; *db/db* = 15. Mice were 12–13 weeks old at the time of testing. $^{*}p \leq 0.05$, $^{**}p \leq 0.01$, $^{***}p \leq 0.001$ vs. control.

n = 4) in prefrontal cortex ($t_{(6)} = 2.451$, $p = 0.0497$; Fig. 5B). The cumulative frequency plot of individual AIS lengths in prefrontal cortex of *db/db* mice showed a leftward shift (Fig. 5C). Similarly, AIS length was shorter (8.8%) in hippocampus of *db/db* mice (24.8 ± 0.68 μm, n = 4) compared with controls (27.19 ± 0.57 μm, n = 3) ($t_{(5)} = 2.572$, $p = 0.0499$; Fig. 5E,F).

3.6. Nodes of Ranvier are disrupted in corpus callosum of 26-week-old db/db mice

To examine nodes of Ranvier in corpus callosum of 26-week-old *db/db* and control mice, we utilized antibodies to Caspr, a paranodal cell adhesion molecule, and neurofascin (NF) 186, a cell adhesion molecule found at nodes [18]. At 26 weeks of age, the nodal gap, or the distance between two paranodal Caspr clusters, was elongated in the corpus callosum of *db/db* mice (1.181 ± 0.031 μm, n = 4) compared with controls (1.040 ± 0.023 μm, n = 4) ($t_{(6)} = 3.642$, $p = 0.0108$; Fig. 6A,B). The length of paranodal Caspr clusters was significantly reduced in *db/db* mice (1.376 ± 0.042 μm, n = 4) compared with controls (1.578 ± 0.035 μm, n = 4) ($t_{(6)} = 3.716$, $p = 0.0099$; Fig. 6C), suggesting that the nodal elongation is caused by partial loss of the paranodal axo-glial junctions.

3.7. MWM spatial learning and flexibility at 24–26 weeks of age

To determine the effects of prolonged type 2 diabetes on cognitive function, we re-tested the mice at 24–26 weeks of age. In accordance with a previous studies [38,42], acquisition showed a main effect of diabetes ($F_{(1, 25.9)} = 71.25$, $p < 0.0001$) and a significant diabetes x day interaction on latency ($F_{(4, 73.7)} = 2.99$, $p = 0.0241$; Fig. 7A). *Db/db* mice also showed a significant effect of diabetes on swim speed ($F_{(1, 22.5)} = 123.17$, $p < 0.0001$), but no significant diabetes x day interaction (Fig. 7B). The *db/db* mice took longer to find the platform and swam slower than control mice. During acquisition, unlike at the younger age (Results Section 3.4), there was a significant diabetes effect on path efficiency ($F_{(1, 29.2)} = 7.83$, $p = 0.0090$) and a diabetes x day interaction ($F_{(4, 72.5)} = 2.98$, $p = 0.0246$). *Db/db* mice were less efficient at finding the platform than controls during the first two days of acquisition (Fig. 7C). Next, we assessed reversal in *db/db* mice. We found a significant effect of diabetes ($F_{(1, 22)} = 204.9$, $p < 0.0001$) and diabetes x day interaction on latency ($F_{(4, 67.8)} = 7.58$, $p < 0.0001$; Fig. 7D). Swim speed showed a main effect of diabetes ($F_{(1, 22.2)} = 212.07$, $p < 0.0001$) with no diabetes x day interaction (Fig. 7E). The *db/db* mice took longer to locate the platform and swam slower than control mice. Path efficiency showed a significant main effect of diabetes ($F_{(1, 22)} = 20.43$, $p = 0.0002$) and the diabetes x day

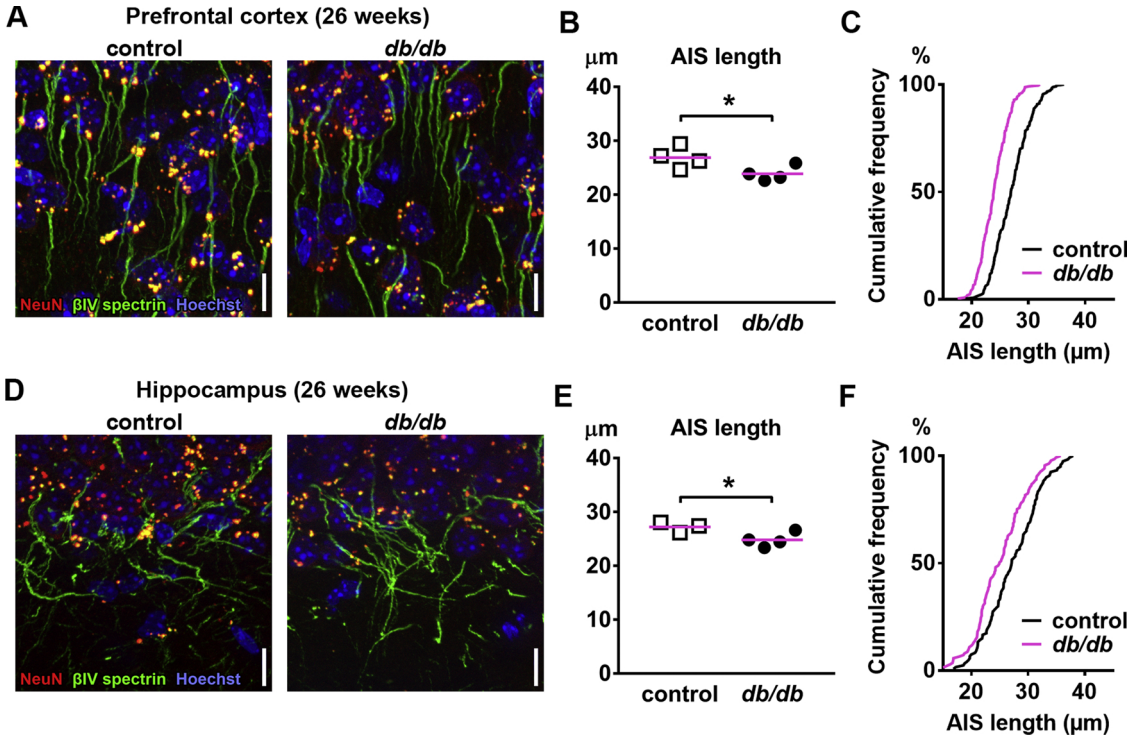

Fig. 5. Type 2 diabetic *db/db* mice have shortened axon initial segment (AIS) in prefrontal cortex and hippocampus at 26 weeks of age. (A) Representative images depicting the prefrontal cortex, prelimbic area, in control (left) and *db/db* (right) mice. Brain sections were labeled for βIV spectrin (green, AIS), NeuN (red, neuronal soma) and Hoechst (blue, cell nuclei). Scale bars = 10 µm. (B) AIS length in prefrontal cortex of 26-week-old *db/db* mice was shorter than lean controls. Mean ± SEM: control = 26.87 ± 1.00 µm; *db/db* = 23.87 ± 0.70 µm. (C) Cumulative frequency distribution plot of AIS lengths in prefrontal cortex shows a leftward shift in *db/db* mice compared with lean controls. Group sizes: control = 4 mice, total 251 AISs; *db/db* = 4 mice, total 254 AISs. (D) Representative images depicting hippocampus, CA1 area, in 26-week-old control (left) and *db/db* (right) mice. Brain sections were labeled for βIV spectrin (green, AIS), NeuN (red, neuronal soma) and Hoechst (blue, cell nuclei). Scale bars = 10 µm. (E) AIS length in hippocampus of 26-week-old *db/db* mice was shorter than lean controls. Mean ± SEM: control = 27.19 ± 0.57 µm; *db/db* = 24.8 ± 0.68 µm. (F) Cumulative frequency distribution plot of AIS lengths in hippocampus shows a slight leftward shift in *db/db* mice compared with lean controls. Group sizes: control = 3 mice, total 120 AISs; *db/db* = 4 mice, total 147 AISs. *$p \leq 0.05$ vs. control.

interaction ($F_{(4,\ 88)} = 5.83$, $p = 0.0003$). There was a significant reduction in path efficiency during days 2–5 (Fig. 7F) compared with only days 4–5 in younger *db/db* mice (Fig. 4F). At the end of reversal in 26-week-old mice, cued-random testing was performed. There was a significant diabetes effect on latency ($F_{(1,\ 22.1)} = 76.41$, $p < 0.0001$; not shown) with *db/db* mice taking longer to reach the cued platform than lean controls.

4. Discussion

For the first time, we report a significant impairment of cognitive flexibility in type 2 diabetic mice. This dysfunction was observed in 13-week-old *db/db* mice after the development of type 2 diabetes [10] and AIS shortening in the prefrontal cortex and hippocampus [28]. At 24–26 weeks of age, we found sustained impairment of cognitive flexibility and AIS shortening, and elongation of nodes of Ranvier in the corpus callosum. Our findings are relevant to cognitive flexibility impairment found in patients with type 2 diabetes and lay the groundwork for future research into structural alteration of excitable axonal domains, such as the AIS and nodes of Ranvier, and its functional implications.

There are a number of pitfalls to assessing cognitive function in diabetic rodents. For example, the attention set-shifting task is widely used to evaluate cognitive flexibility in rodents [43], but food restriction over 3 weeks prior to this test might affect development of diabetes. Previous studies showed decreased locomotor activity in *db/db* mice, and discussed this as a potential confounder of behavioral tasks [35–38], whereas another study reported no hypolocomotion in an open-field in *db/db* mice [44]. In the MWM, the most commonly reported measure of performance is latency to reach the goal, which could be affected by large differences in swim speed. Swim speeds are significantly reduced in *db/db* mice at 10–13 (Figs. 2B, 4 B,E), 18 [45], 24–25 (Fig. 7B,E), and 26 weeks [46]. Although the reason for slower swimming in *db/db* mice is not known, multiple factors such as diabetic polyneuropathy might be involved. Thus, the MWM latency in *db/db* mice may not accurately reflect cognitive function. To avoid these pitfalls in *db/db* mice, we report path efficiency (Figs. 2C, 4 C,F and 7 C,F) in water-based tasks, a measure that does not require food restriction and is not sensitive to changes in locomotor activity, swim speed, or body mass differences [32].

Previous studies and our current results from MWM acquisition show conflicting results of spatial memory deficits in rodent models of type 2 diabetes. ZDF rats did not show spatial learning or memory deficits after 5 or 8 weeks of untreated type 2 diabetes [47]. *Db/db* mice at 7 weeks of age showed a difference only on day-4 of MWM path length with an unadjusted t-test, whereas an overall ANOVA showed no effects on path length [13]. In another study, *db/db* mice at 12 weeks of age had a significantly increased latency compared to control group, although swim speed or path were not assessed [44]. In the present study, we found no difference in path efficiency of 12-week-old *db/db* mice during MWM acquisition (Fig. 4C), suggesting that prolonged latency of the *db/db* mice (Fig. 4A) is mostly due to slow swimming speed (Fig. 4B). *Db/db* mice at 14 weeks of age showed very limited increase of latency, statistically significant only in the last day of the MWM acquisition phase [38]. Impairment of spatial learning and memory in *db/db* mice might be relatively mild at 7–14 weeks of age, which could lead to the observed variation among the studies. At 26 weeks, latency in MWM acquisition was significantly increased along the entire phase

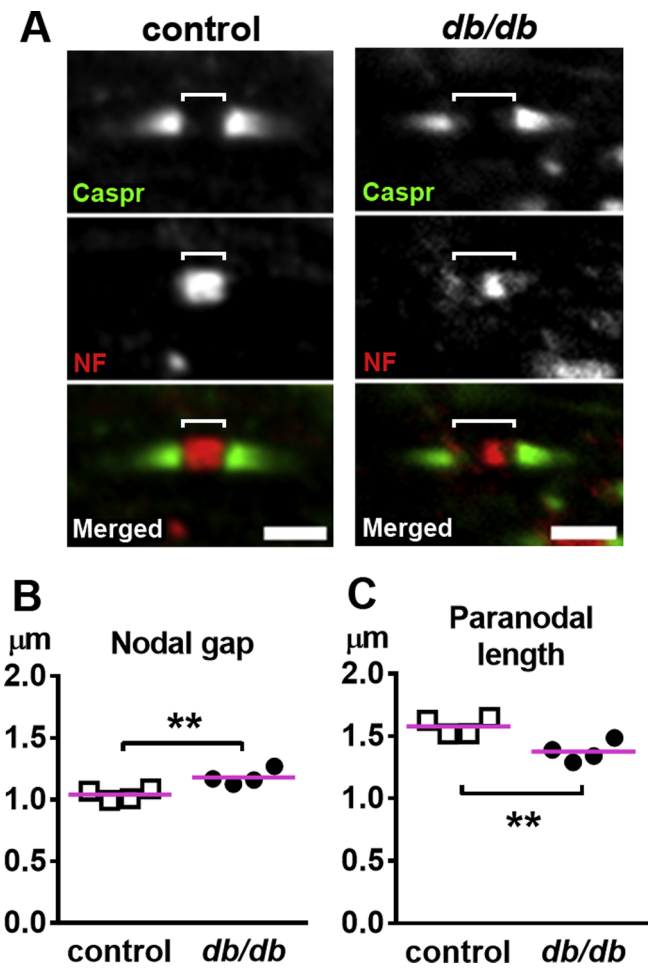

Fig. 6. Node of Ranvier disruption in corpus callosum of 26-week-old *db/db* mice. (A) Representative high magnification images of node of Ranvier in corpus callosum of control (left) and *db/db* (right) mice at 26 weeks of age. Brain sections were labeled for Caspr (green; paranode) and neurofascin (NF; red; node of Ranvier). Brackets depict the nodal gap. Scale bars = 2 µm. (B) The nodal gap, or the distance between two opposing Caspr clusters within the node of Ranvier, was elongated in *db/db* mice. Mean ± SEM: control = 1.040 ± 0.023 µm; *db/db* = 1.181 ± 0.031 µm (500 nodal gaps in each group of n = 4 mice). (C) The length of a single paranodal Caspr cluster was shortened in *db/db* mice. Mean ± SEM: control = 1.578 ± 0.035 µm; *db/db* = 1.376 ± 0.042 µm (1000 paranodes in each group of n = 4 mice). $^{**}p \leq 0.01$ vs. control.

[38] or in 2nd to 4th days [42] in *db/db* mice. In our study, in 24-week-old *db/db* mice, reduced path efficiency in MWM acquisition was observed on days 1 and 2 (Fig. 7C). This might be due to (i) lack of positive transfer of training in *db/db* mice (i.e. control mice retained the memory of previous task, but *db/db* mice did not), or (ii) worsening of *db/db* mouse MWM acquisition performance with age. Although our data do not provide conclusive evidence, both possibilities suggest that *db/db* mice show age-dependent memory disturbance as suggested before [38].

Our current results of decreased path efficiency in MWM reversal at 13 (Fig. 4F) and 25 weeks (Fig. 7F) clearly show impairment of cognitive flexibility in *db/db* mice, whereas we did not find disturbance in working memory (Figs. 2 and 3). Intact executive function, which includes cognitive flexibility [48], is key for successful management of type 2 diabetes. For example, patients with type 2 diabetes need to monitor blood glucose levels while performing other tasks, involving cognitive flexibility [9]. Therefore, impaired cognitive flexibility in patients with type 2 diabetes [5,6] could result in poor diabetes management, which could in-turn exacerbate the impairment of executive function [9] in a vicious positive feedback cycle. Taken together, our findings in *db/db* mice as well as previous observations in patients with type 2 diabetes suggest that cognitive flexibility is one of the critical executive functions affected in the diabetic brain. *Db/db* mice could provide a useful model to test the effects of new treatment strategies to improve executive function during type 2 diabetic condition. To evaluate spatial learning and executive functions in *db/db* mice without the confound of slower swim speeds, future studies should assess path efficiency in MWM acquisition and reversal phases.

The pathophysiology underlying cognitive dysfunction in type 2 diabetes is unknown. Selective disruption of hippocampal cholinergic signaling in mice compromises information processing in the MWM reversal [49], suggesting that impaired cognitive flexibility in *db/db* mice (Figs. 4F, 7 F) could be mediated by changes in the hippocampus. In addition, other brain regions such as prefrontal cortex or striatum may also participate in the modulation of cognitive flexibility (reviewed in [50]). In patients with type 2 diabetes, a previous study [4] suggested that the hippocampus is the first brain site affected, because (i) patients with relatively well-controlled type 2 diabetes of less than 10 years from the time of diagnosis showed deficits in hippocampal-based memory performance while other cognitive domains were preserved; (ii) MRI showed reductions in brain volumes that were restricted to the hippocampus in diabetes patients relative to control subjects; and (iii) there was an inverse relationship between hippocampal volume and HbA1c levels. Another MRI study showed smaller gray matter volumes in the prefrontal lobe in patients with type 2 diabetes when compared with control subjects [51]. Furthermore, functional MRI in patients with type 2 diabetes showed diminished activation in the frontal cortex during working memory tasks [7]. In addition, functional MRI in older adults with type 2 diabetes showed lower resting-state functional connectivity between the hippocampal region and the medial frontal cortex compared with control subjects [52]. Such brain functional changes are likely mediated by changes in neuronal network coordination, which relies on action potential generation (AIS) and propagation (nodes of Ranvier).

In diabetic *db/db* mice, previous studies showed reduced dendritic spine density in the hippocampus [39,53,54] and prefrontal cortex [53], suggesting alterations in neuronal inputs. Our current (Fig. 5) and previous results [28] demonstrate shortening of the AIS, a key structure regulating neuronal outputs, in these brain regions. AIS shortening identified in *db/db* mouse brains (8.8–16%) is functionally relevant, as a computational model showed that AIS length reduction by as little as 1–4% can reduce neuronal excitability [21]. Thus, these structural changes in AIS together with synaptic loss likely disturb the neuronal network coordination presumably required for appropriate cognitive function. Alternatively, AIS shortening could be secondary to other alterations that change neuronal function as a mechanism of homeostatic plasticity. In support of this idea, a computational model suggested that a reduction in AIS length can minimize the threshold current for action potential generation [55]. Future studies are required to determine the functional effects of AIS shortening in diabetic brains. AIS shortening is preventable by managing diabetes [28], suggesting its potential for early intervention. We envision that in both scenarios, therapeutic options could be developed to either inhibit pathology or enhance homeostatic plasticity presented by structural changes in AIS.

In addition to AIS shortening, we observed elongation of nodes of Ranvier along the corpus callosum in 26-week-old *db/db* mice (Fig. 6), but not in 10-week-old mice [28], suggesting that this disruption arises with prolonged diabetes burden. Nodal disruption might be indicative of white matter abnormalities as seen in patients with type 2 diabetes [56], since node assembly and maintenance depends on myelinating oligodendrocytes [17,18]. Indeed, an inverse relationship was observed between executive function and white matter integrity in type 2 diabetes [57,58]. Furthermore, adult-onset metabolic stress in oligodendrocytes causes progressive white matter pathology, AIS shortening in rostral entorhinal cortex, and memory deficits [55]. The nodal and

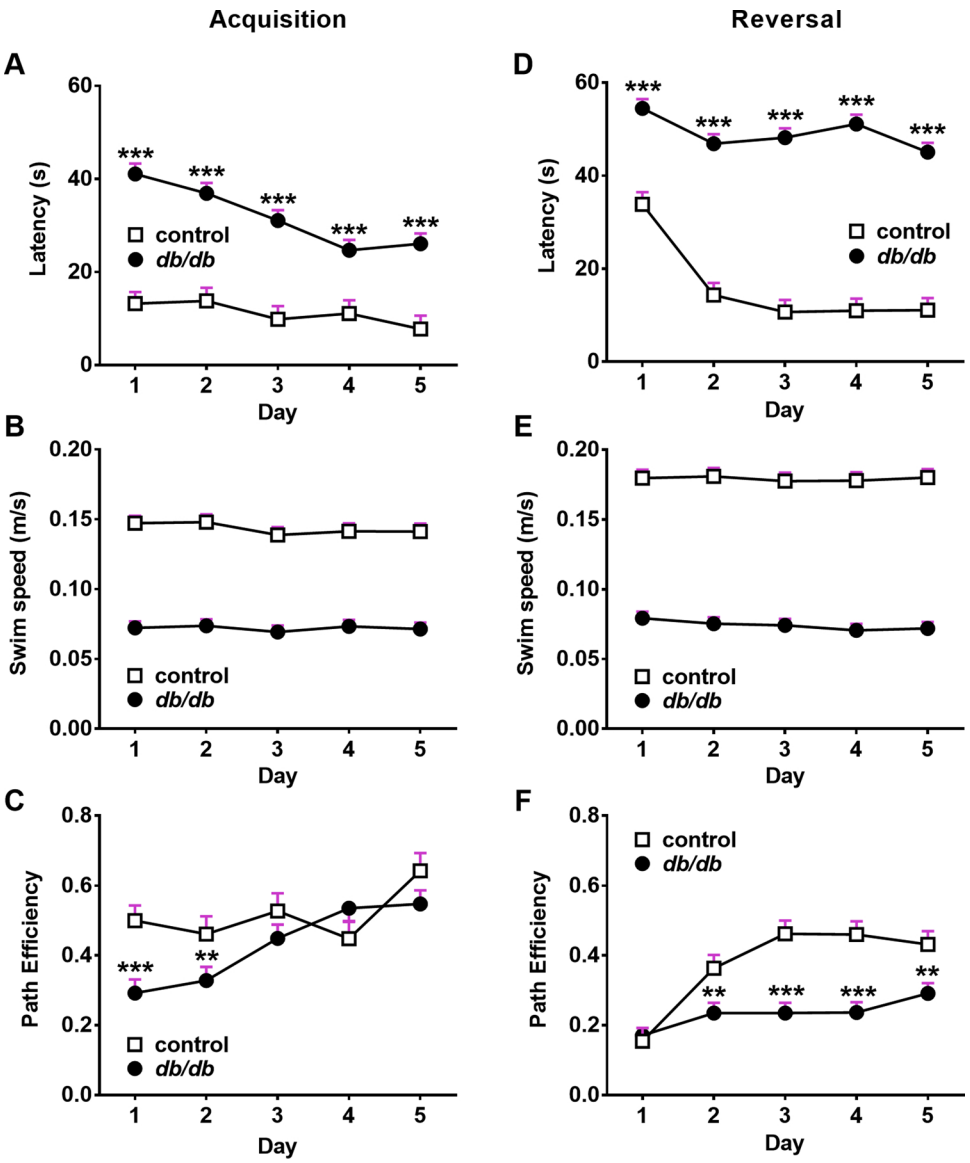

Fig. 7. MWM Acquisition (A–C) and Reversal (D–F). (A) *Db/db* mice had significantly longer latencies to reach the platform than lean controls. (B) Swim speed stayed constant during acquisition. (C) *Db/db* mice were significantly less efficient than lean controls on days 1 and 2. (D) *Db/db* mice had significantly longer latencies to reach the platform than lean controls. (E) Swim speed stayed constant during reversal. (F) Path efficiency was decreased in *db/db* mice compared with lean controls on days 2–5. Data are LS Mean ± SEM. Group sizes: control = 9 (3 controls excluded due to injuries from fighting); *db/db* = 15. Mice were 24–25 weeks old at the time of testing. $^{**}p \leq 0.01$, $^{***}p \leq 0.001$ vs. control.

paranodal abnormalities observed in *db/db* mice (Fig. 6) might explain exacerbated deterioration of cognitive function in older patients [2], since nodal elongation due to paranodal detachment can cause nerve conduction slowing [31]. Similarly, a computational model showed that, when the number of channels was held constant at each node (i.e. reduced density of ion channels at the elongated nodes), the predicted conduction speed fell with increasing node length [59]. In contrast, since nodal elongation might increase conduction speed when the nodal ion channel density is kept constant (i.e. increased number of ion channels at the elongated nodes) [59], we cannot exclude the possibility that nodal elongation is a secondary homeostatic mechanism to offset diabetes-induced nerve conduction slowing due to myelin defects. Future studies are required to determine if nodal elongation is the primary pathology or secondary change, similar to the AIS shortening as discussed above. Nevertheless, our study provides the rationale for future research into excitable axonal domains aimed at mitigating cognitive impairment in patients with type 2 diabetes.

There are many questions that remain to be answered. For example, what is the relationship among alterations in synapses, AIS, nodes, and myelin that culminate in cognitive dysfunction in type 2 diabetes? Furthermore, how does type 2 diabetes lead to AIS shortening and nodal changes? Interestingly, type 2 diabetes is clinically associated with both Alzheimer's disease-type and vascular-type dementias [60], and AIS shortening was reported in mouse models of both Alzheimer's disease [24] and cerebrovascular lesion [61,62]. Some researchers propose that type 2 diabetes and Alzheimer's disease might share metabolic dysfunction upstream of the observed cognitive decline [60]. Such dysfunction likely begins early in the disease process and might explain cognitive decrements observed among type 2 diabetes patients of all ages [2]. Potential metabolic disruptors of axonal domains might include mitochondrial dysfunction [63] or increased glucose metabolite methylglyoxal [64], which were shown to disrupt nodes of Ranvier [65,66], and oxidative stress [67], which induces AIS disruption [68]. Pathological AIS disruption is mediated by overactivation of calcium-dependent protease calpain [68–71], whereas plasticity in AIS structures is mediated via calcium-activated phosphatase calcineurin [72]. Future studies such as time course analyses of these potential mediators in prefrontal cortex and hippocampus could identify the specific mechanisms of disruption of excitable axonal domains in type 2 diabetes. Another important question is whether the lack of functional leptin receptor in *db/db* mice may contribute to axonal domain disruption and cognitive impairment. Leptin signaling plays an important role in neuronal and glial development of mouse embryos [73], as well as in regulation of synaptic function and memory formation in adult animals

[74]. Our previous data suggested that the AIS shortening in *db/db* mice was not due to disrupted leptin signaling, since diabetes treatment ameliorated AIS shortening [28]. However, it is unclear if loss of leptin receptor function contributes to impairment of cognitive flexibility or nodal elongation observed in *db/db* mice. Analyses of other models of type 2 diabetes, such as high-fat diet commonly used to induce insulin resistance in rodents [12], will be helpful to address this issue.

In conclusion, this is the first study to report impaired cognitive flexibility in type 2 diabetic *db/db* mice. We also report AIS shortening and node of Ranvier disruption in these mice. Together these findings highlight impaired cognitive flexibility as a critical component of cognitive dysfunction in type 2 diabetes and identify novel axonal alterations likely to play an important role in disease pathophysiology.

Funding sources

This work was supported by the National Institute of Neurological Disorders and Stroke of the National Institutes of Health under Award Number R56NS107398 (KS).

Declaration of interest

The authors declare no competing financial interests.

Acknowledgements

The authors thank Cameron L. Smith (Department of Neuroscience, Cell Biology and Physiology, Wright State University) for technical assistance, Dr. David Cool (Director of Wright State University Proteome Analysis Laboratory) for the use of the equipment, and Dr. Dragana I. Claflin (Department of Psychology, Wright State University) for critical discussions.

References

[1] L.E. Stoeckel, Z. Arvanitakis, S. Gandy, D. Small, C.R. Kahn, A. Pascual-Leone, A. Pawlyk, R. Sherwin, P. Smith, Complex mechanisms linking neurocognitive dysfunction to insulin resistance and other metabolic dysfunction, F1000Research 5 (2016) 353, https://doi.org/10.12688/f1000research.8300.2.

[2] G.J. Biessels, M.W.J. Strachan, F.L.J. Visseren, L.J. Kappelle, R.A. Whitmer, Dementia and cognitive decline in type 2 diabetes and prediabetic stages: Towards targeted interventions, Lancet Diabetes Endocrinol. 2 (2014) 246–255, https://doi.org/10.1016/S2213-8587(13)70088-3.

[3] P. Palta, A.L.C. Schneider, G.J. Biessels, P. Touradji, F. Hill-Briggs, Magnitude of cognitive dysfunction in adults with type 2 diabetes: a meta-analysis of six cognitive domains and the most frequently reported neuropsychological tests within domains, J. Int. Neuropsychol. Soc. 20 (2014) 278–291, https://doi.org/10.1017/S1355617713001483.

[4] S.M. Gold, I. Dziobek, V. Sweat, A. Tirsi, K. Rogers, H. Bruehl, W. Tsui, S. Richardson, E. Javier, A. Convit, Hippocampal damage and memory impairments as possible early brain complications of type 2 diabetes, Diabetologia 50 (2007) 711–719, https://doi.org/10.1007/s00125-007-0602-7.

[5] H. Thabit, T. Kyaw Tun, J. McDermott, S. Sreenan, Executive function and diabetes mellitus – a stone left unturned? Curr. Diabetes Rev. 8 (2012) 109–115, https://doi.org/10.2174/157339912799424555.

[6] S. Sadanand, R. Balachandar, S. Bharath, Memory and executive functions in persons with type 2 diabetes: a meta-analysis, Diabetes Metab. Res. Rev. 32 (2016) 132–142, https://doi.org/10.1002/dmrr.2664.

[7] Y. Chen, Z. Liu, J. Zhang, K. Xu, S. Zhang, D. Wei, Z. Zhang, Altered brain activation patterns under different working memory loads in patients with type 2 diabetes, Diabetes Care 37 (2014) 3157–3163, https://doi.org/10.2337/dc14-1683.

[8] D.G. Feil, C.W. Zhu, D.L. Sultzer, The relationship between cognitive impairment and diabetes self-management in a population-based community sample of older adults with Type 2 diabetes, J. Behav. Med. 35 (2012) 190–199, https://doi.org/10.1007/s10865-011-9344-6.

[9] S. Black, K. Kraemer, A. Shah, G. Simpson, F. Scogin, A. Smith, Diabetes, depression, and cognition: a recursive cycle of cognitive dysfunction and glycemic dysregulation, Curr. Diab. Rep. 18 (2018) 118, https://doi.org/10.1007/s11892-018-1079-0.

[10] K.P. Hummel, M.M. Dickie, D.L. Coleman, Diabetes, a new mutation in the mouse, Science 153 (1966) 1127–1128, https://doi.org/10.1126/science.153.3740.1127.

[11] R.G. Peterson, W.N. Shaw, M.-A. Neel, L.A. Little, J. Eichberg, Zucker diabetic fatty rat as a model for non-insulin-dependent diabetes mellitus, ILAR J. 32 (1990) 16–19, https://doi.org/10.1093/ilar.32.3.16.

[12] R. Buettner, K.G. Parhofer, M. Woenckhaus, C.E. Wrede, L.A. Kunz-Schughart, J. Schölmerich, L.C. Bollheimer, Defining high-fat-diet rat models: metabolic and molecular effects of different fat types, J. Mol. Endocrinol. 36 (2006) 485–501, https://doi.org/10.1677/jme.1.01909.

[13] X.L. Li, S. Aou, Y. Oomura, N. Hori, K. Fukunaga, T. Hori, Impairment of long-term potentiation and spatial memory in leptin receptor-deficient rodents, Neuroscience 113 (2002) 607–615, https://doi.org/10.1016/S0306-4522(02)00162-8.

[14] C. Gu, W. Zhou, W. Wang, H. Xiang, H. Xu, L. Liang, H. Sui, L. Zhan, X. Lu, ZiBuPiYin recipe improves cognitive decline by regulating gut microbiota in Zucker diabetic fatty rats, Oncotarget 8 (2017) 27693–27703, https://doi.org/10.18632/oncotarget.14611.

[15] A.M. Stranahan, T.V. Arumugam, R.G. Cutler, K. Lee, J.M. Egan, M.P. Mattson, Diabetes impairs hippocampal function through glucocorticoid-mediated effects on new and mature neurons, Nat. Neurosci. 11 (2008) 309–317, https://doi.org/10.1038/nn2055.

[16] Z. Fu, J. Wu, T. Nesil, M.D. Li, K.W. Aylor, Z. Liu, Long-term high-fat diet induces hippocampal microvascular insulin resistance and cognitive dysfunction, Am. J. Physiol. Endocrinol. Metab. 312 (2017) E89–E97, https://doi.org/10.1152/ajpendo.00297.2016.

[17] M.N. Rasband, E. Peles, The nodes of Ranvier: molecular assembly and maintenance, Cold Spring Harb. Perspect. Biol. 8 (2016) a020495, https://doi.org/10.1101/cshperspect.a020495.

[18] R.B. Griggs, L.M. Yermakov, K. Susuki, Formation and disruption of functional domains in myelinated CNS axons, Neurosci. Res. 116 (2017) 77–87, https://doi.org/10.1016/j.neures.2016.09.010.

[19] R. Yamada, H. Kuba, Structural and functional plasticity at the axon initial segment, Front. Cell. Neurosci. 10 (2016) 250, https://doi.org/10.3389/fncel.2016.00250.

[20] N. Jamann, M. Jordan, M. Engelhardt, Activity-dependent axonal plasticity in sensory systems, Neuroscience 368 (2018) 268–282, https://doi.org/10.1016/j.neuroscience.2017.07.035.

[21] K.L. Baalman, R.J. Cotton, S.N. Rasband, M.N. Rasband, Blast wave exposure impairs memory and decreases axon initial segment length, J. Neurotrauma 30 (2013) 741–751, https://doi.org/10.1089/neu.2012.2478.

[22] K.C. Clark, A. Josephson, S.D. Benusa, R.K. Hartley, M. Baer, S. Thummala, M. Joslyn, B.A. Sword, H. Elford, U. Oh, A. Dilsizoglu-Senol, C. Lubetzki, M. Davenne, G.H. DeVries, J.L. Dupree, Compromised axon initial segment integrity in EAE is preceded by microglial reactivity and contact, Glia 64 (2016) 1190–1209, https://doi.org/10.1002/glia.22991.

[23] R. Aharoni, N. Schottlender, D.D. Bar-Lev, R. Eilam, M. Sela, M. Tsoory, R. Arnon, Cognitive impairment in an animal model of multiple sclerosis and its amelioration by glatiramer acetate, Sci. Rep. 9 (2019) 4140, https://doi.org/10.1038/s41598-019-40713-4.

[24] M.A. Marin, J. Ziburkus, J. Jankowsky, M.N. Rasband, Amyloid-β plaques disrupt axon initial segments, Exp. Neurol. 281 (2016) 93–98, https://doi.org/10.1016/j.expneurol.2016.04.018.

[25] M.J. Craner, A.C. Lo, J.A. Black, S.G. Waxman, Abnormal sodium channel distribution in optic nerve axons in a model of inflammatory, demyelination Brain. 126 (2003) 1552–1561, https://doi.org/10.1093/brain/awg153.

[26] J.D. Hinman, A. Peters, H. Cabral, D.L. Rosene, W. Hollander, M.N. Rasband, C.R. Abraham, Age-related molecular reorganization at the node of Ranvier, J. Comp. Neurol. 495 (2006) 351–362, https://doi.org/10.1002/cne.20886.

[27] I. Sugiyama, K. Tanaka, M. Akita, K. Yoshida, T. Kawase, H. Asou, Ultrastructural analysis of the paranodal junction of myelinated fibers in 31-month-old-rats, J. Neurosci. Res. 70 (2002) 309–317, https://doi.org/10.1002/jnr.10386.

[28] L.M. Yermakov, D.E. Drouet, R.B. Griggs, K.M. Elased, K. Susuki, Type 2 Diabetes Leads to Axon Initial Segment Shortening in *db/db* Mice, Front. Cell. Neurosci. 12 (2018) 146, https://doi.org/10.3389/fncel.2018.00146.

[29] H. Chen, O. Charlat, L.A. Tartaglia, E.A. Woolf, X. Weng, S.J. Ellis, N.D. Lakey, J. Culpepper, K.J. More, R.E. Breitbart, G.M. Duyk, R.I. Tepper, J.P. Morgenstern, Evidence that the diabetes gene encodes the leptin receptor: Identification of a mutation in the leptin receptor gene in *db/db* mice, Cell 84 (1996) 491–495, https://doi.org/10.1016/S0092-8674(00)81294-5.

[30] D.L. Coleman, K.P. Hummel, Hyperinsulinemia in pre-weaning diabetes (*db*) mice, Diabetologia 10 (Suppl) (1974) 607–610.

[31] C.F. Babbs, R. Shi, Subtle paranodal injury slows impulse conduction in a mathematical model of myelinated axons, PLoS One 8 (2013) e67767, https://doi.org/10.1371/journal.pone.0067767.

[32] C.V. Vorhees, M.T. Williams, Morris water maze: procedures for assessing spatial and related forms of learning and memory, Nat. Protoc. 1 (2006) 848–858, https://doi.org/10.1038/nprot.2006.116.

[33] L.A. Hyde, B.J. Hoplight, V.H. Denenberg, Water version of the radial-arm maze: learning in three inbred strains of mice, Brain Res. 785 (1998) 236–244, https://doi.org/10.1016/S0006-8993(97)01417-0.

[34] J. Schindelin, I. Arganda-Carreras, E. Frise, V. Kaynig, M. Longair, T. Pietzsch, S. Preibisch, C. Rueden, S. Saalfeld, B. Schmid, J.Y. Tinevez, D.J. White, V. Hartenstein, K. Eliceiri, P. Tomancak, A. Cardona, Fiji: an open-source platform for biological-image analysis, Nat. Methods 9 (2012) 676–682, https://doi.org/10.1038/nmeth.2019.

[35] A.N. Sharma, K.M. Elased, T.L. Garrett, J.B. Lucot, Neurobehavioral deficits in *db/db* diabetic mice, Physiol. Behav. 101 (2010) 381–388, https://doi.org/10.1016/j.physbeh.2010.07.002.

[36] A.N. Sharma, K.M. Elased, J.B. Lucot, Rosiglitazone treatment reversed depression-but not psychosis-like behavior of *db/db* diabetic mice, J. Psychopharmacol. 26 (2012) 724–732, https://doi.org/10.1177/0269881111434620.

[37] M. Guo, X.Y. Lu, Leptin receptor deficiency confers resistance to behavioral effects of fluoxetine and desipramine via separable substrates, Transl. Psychiatry 4 (2014) e486, https://doi.org/10.1038/tp.2014.126.

[38] J.J. Ramos-Rodriguez, O. Ortiz, M. Jimenez-Palomares, K.R. Kay, E. Berrocoso, M.I. Murillo-Carretero, G. Perdomo, T. Spires-Jones, I. Cozar-Castellano, A.M. Lechuga-Sancho, M. Garcia-Alloza, Differential central pathology and cognitive impairment in pre-diabetic and diabetic mice, Psychoneuroendocrinology 38 (2013) 2462–2475, https://doi.org/10.1016/j.psyneuen.2013.05.010.

[39] A.M. Stranahan, K. Lee, B. Martin, S. Maudsley, E. Golden, R.G. Cutler, M.P. Mattson, Voluntary exercise and caloric restriction enhance hippocampal dendritic spine density and BDNF levels in diabetic mice, Hippocampus 19 (2009) 951–961, https://doi.org/10.1002/hipo.20577.

[40] M.R. Skelton, T.L. Schaefer, N.R. Herring, C.E. Grace, C.V. Vorhees, M.T. Williams, Comparison of the developmental effects of 5-methoxy-N,N-diisopropyltryptamine (Foxy) to (+/-)-3,4-methylenedioxymethamphetamine (ecstasy) in rats, Psychopharmacology (Berl.) 204 (2009) 287–297, https://doi.org/10.1007/s00213-009-1459-x.

[41] Y. Cui, J. Jin, X. Zhang, H. Xu, L. Yang, D. Du, Q. Zeng, J.Z. Tsien, H. Yu, X. Cao, Forebrain NR2B overexpression facilitating the prefrontal cortex long-term potentiation and enhancing working memory function in mice, PLoSOne 6 (2011) e20312, https://doi.org/10.1371/journal.pone.0020312.

[42] D. Pu, Y. Zhao, J. Chen, Y. Sun, A. Lv, S. Zhu, C. Luo, K. Zhao, Q. Xiao, Protective effects of sulforaphane on cognitive impairments and AD-like lesions in diabetic mice are associated with the upregulation of Nrf2 transcription activity, Neuroscience 381 (2018) 35–45, https://doi.org/10.1016/j.neuroscience.2018.04.017.

[43] S. Shiers, G. Pradhan, J. Mwirigi, G. Mejia, A. Ahmad, S. Kroener, T. Price, Neuropathic pain creates an enduring prefrontal cortex dysfunction corrected by the type II diabetic drug metformin but not by gabapentin, J. Neurosci. 38 (2018) 7337–7350, https://doi.org/10.1080/00288233.1960.10418075.

[44] H. Wang, F. Chen, K.L. Zhong, S.S. Tang, M. Hu, Y. Long, M.X. Miao, J.M. Liao, H.B. Sun, H. Hong, PPARγ agonists regulate bidirectional transport of amyloid-β across the blood-brain barrier and hippocampus plasticity in *db / db* mice, Br. J. Pharmacol. 173 (2016) 372–385, https://doi.org/10.1111/bph.13378.

[45] Q. Zhao, K. Matsumoto, K. Tsuneyama, K. Tanaka, F. Li, N. Shibahara, T. Miyata, T. Yokozawa, Diabetes-induced central cholinergic neuronal loss and cognitive deficit are attenuated by tacrine and a Chinese herbal prescription, Kangen-karyu: elucidation in type 2 diabetes db/db mice, J. Pharmacol. Sci. 117 (2011) 230–242, https://doi.org/10.1254/jphs.11115FP.

[46] C. Infante-Garcia, J. Jose Ramos-Rodriguez, Y. Marin-Zambrana, M. Teresa Fernandez-Ponce, L. Casas, C. Mantell, M. Garcia-Alloza, Mango leaf extract improves central pathology and cognitive impairment in a type 2 diabetes mouse model, Brain Pathol. 27 (2017) 499–507, https://doi.org/10.1111/bpa.12433.

[47] A. Bélanger, N. Lavoie, F. Trudeau, G. Massicotte, S. Gagnon, Preserved LTP and water maze learning in hyperglycaemic-hyperinsulinemic ZDF rats, Physiol. Behav. 83 (2004) 483–494, https://doi.org/10.1016/j.physbeh.2004.08.031.

[48] S. Funahashi, J.M. Andreau, Prefrontal cortex and neural mechanisms of executive function, J. Physiol. Paris 107 (2013) 471–482, https://doi.org/10.1016/j.jphysparis.2013.05.001.

[49] M.A. Al-Onaizi, G.M. Parfitt, B. Kolisnyk, C.S.H. Law, M.S. Guzman, D.M. Barros, L.S. Leung, M.A.M. Prado, V.F. Prado, Regulation of cognitive processing by hippocampal cholinergic tone, Cereb. Cortex 27 (2017) 1615–1628, https://doi.org/10.1093/cercor/bhv349.

[50] V.F. Prado, H. Janickova, M.A. Al-Onaizi, M.A.M. Prado, Cholinergic circuits in cognitive flexibility, Neuroscience 345 (2017) 130–141, https://doi.org/10.1016/j.neuroscience.2016.09.013.

[51] A. Kumar, E. Haroon, C. Darwin, D. Pham, O. Ajilore, G. Rodriguez, J. Mintz, Gray matter prefrontal changes in type 2 diabetes detected using MRI, J. Magn. Reson. Imaging 27 (2008) 14–19, https://doi.org/10.1002/jmri.21224.

[52] H. Zhang, Y. Hao, B. Manor, P. Novak, W. Milberg, J. Zhang, J. Fang, V. Novak, Intranasal insulin enhanced resting-state functional connectivity of hippocampal regions in type 2 diabetes, Diabetes 64 (2015) 1025–1034, https://doi.org/10.2337/db14-1000.

[53] J. Chen, L. Liang, L. Zhan, Y. Zhou, L. Zheng, X. Sun, J. Gong, H. Sui, R. Jiang, F. Zhang, L. Zhang, ZiBuPiYin recipe protects db/db mice from diabetes-associated cognitive decline through improving multiple pathological changes, PLoS One 9 (2014) e91680, https://doi.org/10.1371/journal.pone.0091680.

[54] M. Dhar, M. Zhu, S. Impey, T.J. Lambert, T. Bland, I.N. Karatsoreos, T. Nakazawa, S.M. Appleyard, G.A. Wayman, Leptin induces hippocampal synaptogenesis via CREB-Regulated MicroRNA-132 suppression of p250GAP, Mol. Endocrinol. 28 (2014) 1073–1087, https://doi.org/10.1210/me.2013-1332.

[55] D.Z. Radecki, E.L. Johnson, A.K. Brown, N.T. Meshkin, S.A. Perrine, A. Gow, Corticohippocampal dysfunction in the OBiden mouse model of primary oligodendrogliopathy, Sci. Rep. 8 (2018) 16116, https://doi.org/10.1038/s41598-018-34414-7.

[56] J.L. Hsu, Y.L. Chen, J.G. Leu, F.S. Jaw, C.H. Lee, Y.F. Tsai, C.Y. Hsu, C.H. Bai, A. Leemans, Microstructural white matter abnormalities in type 2 diabetes mellitus: a diffusion tensor imaging study, Neuroimage 59 (2012) 1098–1105, https://doi.org/10.1016/j.neuroimage.2011.09.041.

[57] J. Zhang, Y. Wang, J. Wang, X. Zhou, N. Shu, Y. Wang, Z. Zhang, White matter integrity disruptions associated with cognitive impairments in type 2 diabetic patients, Diabetes 63 (2014) 3596–3605, https://doi.org/10.2337/db14-0342.

[58] S.M. Manschot, A.M.A. Brands, J. Van Der Grond, R.P.C. Kessels, A. Algra, L.J. Kappelle, G.J. Biessels, Brain magnetic resonance imaging correlates of impaired cognition in patients with type 2 diabetes, Diabetes 55 (2006) 1106–1113, https://doi.org/10.2337/diabetes.55.04.06.db05-1323.

[59] I.L. Arancibia-Cárcamo, M.C. Ford, L. Cossell, K. Ishida, K. Tohyama, D. Attwell, Node of Ranvier length as a potential regulator of myelinated axon conduction speed, eLife 6 (2017), https://doi.org/10.7554/eLife.23329.

[60] Y. Chornenkyy, W.X. Wang, A. Wei, P.T. Nelson, Alzheimer's disease and type 2 diabetes mellitus are distinct diseases with potential overlapping metabolic dysfunction upstream of observed cognitive decline, Brain Pathol. 29 (2018) 3–17, https://doi.org/10.1111/bpa.12655.

[61] J.D. Hinman, M.N. Rasband, S.T. Carmichael, Remodeling of the axon initial segment after focal cortical and white matter stroke, Stroke 44 (2013) 182–189, https://doi.org/10.1161/STROKEAHA.112.668749.

[62] H. Coban, S. Tung, B. Yoo, H.V. Vinters, J.D. Hinman, Molecular disorganization of axons adjacent to human cortical microinfarcts, Front. Neurol. 8 (2017) 405, https://doi.org/10.1007/s00424-009-0722-7.

[63] B.J. Neth, S. Craft, Insulin resistance and Alzheimer's disease: bioenergetic linkages, Front. Aging Neurosci. 9 (2017) 345, https://doi.org/10.3389/fnagi.2017.00345.

[64] A. Bierhaus, T. Fleming, S. Stoyanov, A. Leffler, A. Babes, C. Neacsu, S.K. Sauer, M. Eberhardt, M. Schnölzer, F. Lasischka, W.L. Neuhuber, T.I. Kichko, I. Konrade, R. Elvert, W. Mier, V. Pirags, I.K. Lukic, M. Morcos, T. Dehmer, N. Rabbani, P.J. Thornalley, D. Edelstein, C. Nau, J. Forbes, P.M. Humpert, M. Schwaninger, D. Ziegler, D.M. Stern, M.E. Cooper, U. Haberkorn, M. Brownlee, P.W. Reeh, P.P. Nawroth, Methylglyoxal modification of Na v 1.8 facilitates nociceptive neuron firing and causes hyperalgesia in diabetic neuropathy, Nat. Med. 18 (2012) 926–933, https://doi.org/10.1038/nm.2750.

[65] M. Marella, G. Patki, A. Matsuno-Yagi, T. Yagi, Complex I inhibition in the visual pathway induces disorganization of the node of Ranvier, Neurobiol. Dis. 58 (2013) 281–288, https://doi.org/10.1016/j.nbd.2013.06.010.

[66] R.B. Griggs, L.M. Yermakov, D.E. Drouet, D.V.M. Nguyen, K. Susuki, Methylglyoxal disrupts paranodal axoglial junctions via calpain activation, ASN Neuro 10 (2018) 175909141876617, https://doi.org/10.1177/1759091418766175.

[67] N. Verma, H. Ly, M. Liu, J. Chen, H. Zhu, M. Chow, L.B. Hersh, F. Despa, Intraneuronal amylin deposition, peroxidative membrane injury and increased IL-1β synthesis in brains of Alzheimer's disease patients with type-2 diabetes and in diabetic HIP rats, J. Alzheimers Dis. 53 (2016) 259–272, https://doi.org/10.3233/JAD-160047.

[68] K.C. Clark, B.A. Sword, J.L. Dupree, Oxidative stress induces disruption of the axon initial segment, ASN Neuro 9 (2017) 1759091417745426, https://doi.org/10.1177/1759091417745426.

[69] D.P. Schafer, S. Jha, F. Liu, T. Akella, L.D. McCullough, M.N. Rasband, Disruption of the axon initial segment cytoskeleton is a new mechanism for neuronal injury, J. Neurosci. 29 (2009) 13242–13254, https://doi.org/10.1523/JNEUROSCI.3376-09.2009.

[70] A. del Puerto, L. Fronzaroli-Molinieres, M.J. Perez-Alvarez, P. Giraud, E. Carlier, F. Wandosell, D. Debanne, J.J. Garrido, ATP-P2X7 receptor modulates axon initial segment composition and function in physiological conditions and brain injury, Cereb. Cortex 25 (2015) 2282–2294, https://doi.org/10.1093/cercor/bhu035.

[71] T. Benned-Jensen, R.K. Christensen, F. Denti, J.-F. Perrier, H.B. Rasmussen, S.-P. Olesen, Live imaging of Kv7.2/7.3 cell surface dynamics at the axon initial segment: high steady-state stability and calpain-dependent excitotoxic down-regulation revealed, J. Neurosci. 36 (2016) 2261–2266, https://doi.org/10.1523/JNEUROSCI.2631-15.2016.

[72] M.D. Evans, A.S. Dumitrescu, D.L.H. Kruijssen, S.E. Taylor, M.S. Grubb, Rapid modulation of axon initial segment length influences repetitive spike firing, Cell Rep. 13 (2015) 1233–1245, https://doi.org/10.1016/j.celrep.2015.09.066.

[73] J. Udagawa, R. Hashimoto, H. Suzuki, T. Hatta, Y. Sotomaru, K. Hioki, Y. Kagohashi, T. Nomura, Y. Minami, H. Otani, The role of leptin in the development of the cerebral cortex in mouse embryos, Endocrinology 147 (2006) 647–658, https://doi.org/10.1210/en.2005-0791.

[74] W. Pan, H. Hsuchou, B. Jayaram, R.S. Khan, E.Y.K. Huang, X. Wu, C. Chen, A.J. Kastin, Leptin action on nonneuronal cells in the CNS: potential clinical applications, Ann. N. Y. Acad. Sci. 1264 (2012) 64–71, https://doi.org/10.1111/j.1749-6632.2012.06472.x.